Validation of a numerical-experimental methodology for structural health monitoring on automotive components

VALIDATION OF A NUMERICAL-EXPERIMENTAL METHODOLOGY FOR STRUCTURAL HEALTH MONITORING ON AUTOMOTIVE COMPONENTS

Lorenzo Sisca
Politecnico di Torino - Italy

Alessandro Messana
Politecnico di Torino - Italy

Henrique de Carvalho Pinheiro
Politecnico di Torino - Italy

Alessandro Ferraris
Beond s.r.l. Torino - Italy

Andrea Giancarlo Airale
Beond s.r.l. Torino - Italy

Massimiliana Carello
Politecnico di Torino - Italy

ABSTRACT

In the recent years, the materials composing the traditional of aircrafts are being progressively replaced with lower density materials, as the Reinforced Plastics. The same trend has been highlighted in the Automotive field to assess the reduction of fuel consumption and CO2 emission.

In order to achieve an optimization of maintenance a variety of on-board systems has been applied for on-line SHM based on piezoelectric transducers earned a particularly high interest for continuous monitoring on metallic and composite structures. The application of this system in automotive could enhance passenger safety, through the monitoring of the vehicle composite material structure health status.

In this paper, six mathematical models for evaluating the electrical response of piezoelectric sensors have been implemented, with the aim of selecting the most effective model for damage identification. Experimental tests were carried out on three types of simpler specimens of different geometries made of different materials (steel, aluminum and carbon fiber). A correlation study has been carried on in order to support the positioning of sensors.

The proposed numerical-experimental methodology is an essential foundation for the introduction of monitoring systems based on piezoelectric transducers in the Automotive sector.

Keywords: Structural Health Monitoring, Automotive, Carbon Fiber Composites, Piezoelectric Transducers, Environmental Operating Conditions

NOMENCLATURE

BASELINE	Experimental condition of specimen for initial data acquisition
BEND	Experimental condition of specimen in bending loading
CCA	Damage Index based on Maximum of the correlation
CC0	Damage Index based on Zero-lag correlation
CRC	Damage Index based on Correlation coefficient
CFRP	Carbon Fiber Reinforced Plastic
DAM	Condition of specimen with Damage
DI	Damage Index
ENV	Damage Index based on Maximum envelope of the difference
EOCs	Environmental Operating Conditions
FEM	Finite Element Method
FEA	Finite Element Analysis
IEHV	Innovative Electric and Hybrid Vehicles
IP	Intellectual Property
MA	Damage Index based on Maximum amplitude of the difference
NRE	Damage Index based on Normalized residual energy
PIEZO	Piezoelectric Transducer
PZT	Piezoelectric Transducer
SHM	Structural Health Monitoring
TEST	Experimental condition of specimen for current data acquisition

INTRODUCTION

Nowadays in all application fields, the evolution about the materials regards the integration of several sensors to continuously assess the conditions of the structure. The need of knowledge about the health condition of the so-called Smart Structures is reasonable, proportionally to the safety and reliability requirements to be assessed [1]. The technical names to describe the verification of the Smart Structures are “Structural Health Monitoring”, “Condition Monitoring” or “Fault Detection”.

Although the SHM presents itself as mature and widespread in many sectors, the structural applications related to the automotive field are not, where the presence of SHM is limited to niche and very specific cases, not reaching the market in relevant levels. This is clearly mirrored to the availability of patents and IP protection related to this field. The geographical distribution of the applications has a big concentration in terms of number of patents in China, followed by the US and other developed countries such as Korea, UK, Japan and Germany. In the last couple of decades the number of new patents filled a year has a growing trend, correlated with the relevance of the field.

The materials applied on the aircrafts are mainly the traditional metals, steel, aluminum, but in recent years they are progressively replaced with lower density materials, as the Reinforced Plastics. The same trend has highlighted in the Automotive field to assess the reduction of fuel consumption and CO2 emission [2,3,4]. It is known that the polymer composites have outstanding properties of specific modulus and strength respect to the low density but suffer more than metals from damage generation and propagation.

Since not all inspection techniques are applicable on a structure for continuous monitoring and some of them are not suitable for composite materials, the best candidates for lightweight, conformability and large area covered are Optical Fibers, Acoustic Emission and Lamb Waves [5]. The Lamb Waves method is based on piezoelectric transducers that work as actuators and sensors in the acousto-ultrasonic regime. They give the possibility to monitor the condition of specific areas of the structure, positioning the transducers only on the most safety-critical positions [6]. The SHM based on guided waves takes advantage of the propagation behavior of particular waves inside the materials. While the traditional Ultrasonic Non-Destructive Testing study the bulk section of the structure, the Guided waves are able to inspect large area thanks to surface propagation [7].

Within the several types of Guided waves, the most common are Lamb waves, that propagates on the surface of thin plates and shells in the frequency range 10-500 kHz. The piezoelectric transducers, due to the possibility to act as actuators and sensors, are used to excite the structure at this frequency regime and measure the vibrational response of the structure. The presence of a defect or a damage is found comparing the final response with the initial baseline of the electrical signal measured by the sensors, repeating the same excitation signal from the actuator piezo. The common signal for SHM applications is a 5 sines burst with a Hanning modulation [8].

For SHM application, the most common format of the piezoelectric transducers is the disc shape [9,10], although some rectangular formats are also applied for dynamic actuation [8]. In case of large plates, the geometrical disposition of piezo can be square, circular or hexagonal [9]. These configurations are suitable for the investigation of the propagation behavior of Lamb waves on the structure in different directions, especially for composite materials. The interaction with an artificial damage is analyzed, when the damage is introduced in the center of piezoelectric network as a notch or a growing fatigue crack [11]. The validation of monitoring systems passes through prototypes near to application scale, as for parts of aircraft wing [9]. The SHM may detect false positives related to ambient variable change instead of real damage. The laboratory specimen has, therefore, to reproduce the external conditions to analyze the response of the SHM system in the Environmental Operating Conditions (EOCs), such as structural loading and temperature/humidity [6,7,12].

Theoretical formulations are able to numerically simulate the possible wave modes generated on a specific structure and some commercial tools allow to represent the piezoelectric elements with different methodologies. The waves propagation on a carbon fiber structure have been studied using LS-DYNA to evaluate the waves interaction with the stiffener [9]. Recently, material cards specific for piezoelectric simulation have been introduced on ABAQUS, able to reproduce the electro-mechanical coupling with the structure and the electrical potential load for piezo actuators. These functions allow to model the system more in detail with the benefits of good fitting with the experimental signals, but increasing the computational time.

MATERIALS AND METHODS

2.1 Specimens

The materials more commonly investigated for SHM trials are steel, aluminum and composite materials based on Carbon Fiber [8,9]. The proposed methodology is based on testing the specimens described in made of these three materials, as represented in Figure 1. The different geometries, number of piezoelectric transducers used, combination of test configurations and loading cases are considered with customized specimens increasing in complexity to reach the wider knowledge of the system response. The vibrational wave on the path contains the information about the structural integrity of the component, as schematized in Figure 1.

a) 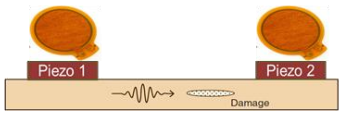

b) 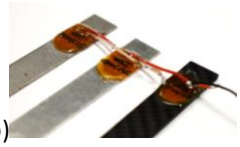

FIGURE 1: a) PIEZOELECTRIC COUPLE WORKING ON A DAMAGED STRUCTURE, b) EXAMPLE OF PIEZO GLUED ON SPECIMENS MADE OF THREE MATERIALS

The Beam specimen is a thin and narrow rectangular plate of 300x12 mm, where the guided waves are constrained to move from the source in the longitudinal direction. The artificial damage is placed in the center between actuator and sensors, as represented in Figure 2. The configurations tested are: Appended to test the specimen in free mode and Clamped at one edge to reduce the free path of the waves.

a) 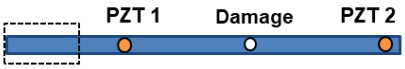

b) 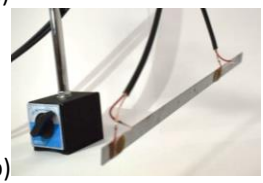
c) 

FIGURE 2: a) SCHEME OF BEAM, b) APPENDED AND c) CLAMPED TEST CONFIGURATIONS

The Plate specimen is a square plate of 250 mm side. As presented in Figure 3, the tested configuration for three materials is only positioned on the table to avoid issues of appending or clamping. Four piezoelectric patches are placed in the middle of each side forming a symmetrical network. The artificial damage is placed in the quadrant of piezo 1 and piezo 2 on the diagonal.

a) 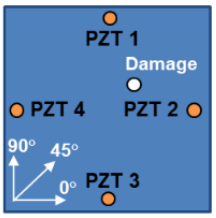

b) 

FIGURE 3: a) SCHEME OF PLATE, b) ON TABLE TEST CONFIGURATION

The simulacrum is a rectangular plate of 250x70 mm and has been designed to pass from a non-stressed specimen to a loaded component, since the bending of a plate is the preferred loading configuration for the validation of prototypal systems, as crack monitoring with piezoelectric elements [13]. The evaluation of SHM system is made both in the unloaded and loaded static conditions, with the fixture reported in Figure 4. The piezo actuator is placed in the center of the top face, the 1st sensor is on the same face but over the upper support, in order to study the attenuation under loading. The 2nd sensor is mounted on the bottom face exactly under the actuator, to evaluate the waves propagation in the thickness.

The bending load on the simulacrum specimen is analyzed through the measurement of strain in two zones of the face in tension thanks to the use of strain gauges (SG 1, SG 2). The positions are chosen to be respectively in the center of the specimen and under the upper support.

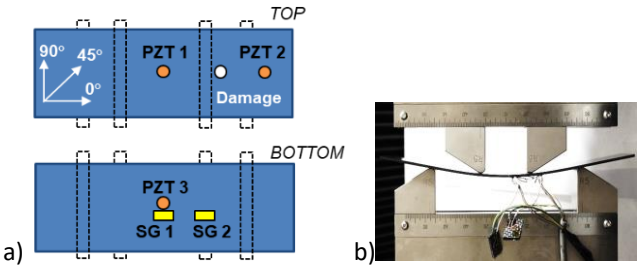

FIGURE 4: a) SCHEME OF SIMULACRUM, b) BENDING TEST CONFIGURATION

Due to easiness and repeatability, two different artificial damages have been produced obtaining the profiles showed in Figure 5. The first damage a) and c) is a non-passing indentation of 2 mm diameter on the surface of specimen, representing a surface defect on the structure. The second damage b) and d) is a passing hole of 4 mm, representing a volume defect in the structure.

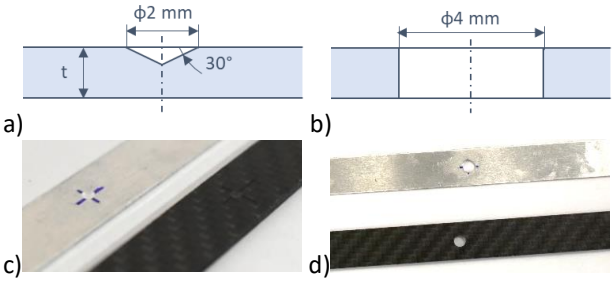

FIGURE 5: a) SCHEME OF DAMAGE 1 AND b) DAMAGE 2, IMAGES OF c) DAMAGE 1 AND d) DAMAGE 2

2.2 Experimental Test Setup

In this research, the circular Piezoelectric transducer PI DuraActTM P-876K025 has been used with material PIC255 (modified Lead Zirconate-Lead Titanate), Piezoceramic disk φ10 mm and thickness 0,2 mm, total thickness of 0,5 mm. The control of Piezoelectric transducers, working as actuators or sensors, has been properly made using the National Instruments Multifunction DAQ NI USB-6259 that has been controlled with a properly made MatLab code.

The response signal of the sensor is highly dependent from the type of the excitation signal chosen for the actuator. The shape for the burst for this work is a 5 sines Hanning-windowed modulated signal with a Voltage Amplitude of 20 Vpp. The transducer Piezo 1 is always the actuator and the Piezo 2, 3 and 4 are the sensors.

The four-point bending tests for characterizing the simulacrum specimens have been realized at crosshead speed of 2 mm/min with an inner supports span of 80 mm and an outer span of 160 mm on the universal testing machine Shimadzu AG-X Plus equipped with a 300 kN load cell. The deformation on the simulacrum specimens and on the leaf spring component has been measured using the HBK 350 Ω strain gauges. The signal from Wheatstone quarter bridge type II has been amplified with a data acquisition module (HBK QuantumX MX1615B) at 10 Hz of sampling rate.

The force vs. displacement and force vs. strain curves are reported in Figure 6. In correspondence of 1000 N for steel and 500 N for aluminum, it has been identified a deviation from linearity for the second strain gauge (SG 2). For this reason, to study all the simulacrum specimens in the same elastic behavior, it has been chosen three loading steps at 0 mm, 0.3 mm and 0.6 mm for the validation of SHM methodology on the stressed structures.

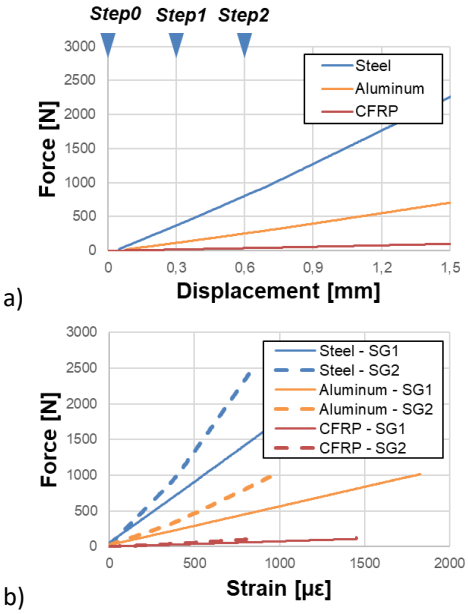

FIGURE 6: BENDING TEST RESULTS ON SIMULACRUM: a) FORCE VS. DISPLACEMENT, b) FORCE VS. STRAIN

2.3 Data Analysis

The aim of data processing in SHM systems is the conversion of complex signals to a simple quantitative variable, that allows the users to understand the health condition of the structure [7,14].

The SHM system developed is based on the data acquisition from one sensor each time, avoiding the reduction of the sample rate due to synchronous input channels from different piezo sensors. The total time of acquisition is 10 times longer than the time of burst, that depends on the frequency. The acquisition with the same piezo couple is repeated 10 times for statistical analysis.

The drift of the piezoelectric signal is digitally corrected using a MatLab function called “detrend”. After the detrend, a low-pass filter is applied on the signal and the cut frequency is the same of the actuation signal.

Since the SHM uses a property of Lamb waves to interact with damages in the structure, it is not possible to select a priori the best frequency for specific specimens, geometries, materials and piezo disposition. For this reason, it has been individuated the range of frequencies 1-100 kHz with step of 1 kHz and for each frequency the procedure explained in the previous paragraph has been applied.

The presence of damages or changes in the structure can be detected observing the response signal of the piezoelectric sensor. The evaluation of the results at the 100 frequencies is possible with the visualization on spectrogram, in particular the frequency vs. time as a function of voltage (color scale) [15]. Figure 7 reports the visualization of the excitation signal of piezo 1 in the entire frequency range.

The configuration of the structure “as it is” without defects and damages is called “BASE” or “ Baseline”, while the configuration to compare with the Baseline is called “TEST” and can be damaged or stressed (e.g. Test 1 and Test 2 are configurations for two incremental damages or bending loads).

The thicker yellow and blue lines refer respectively to the positive and negative peaks of Voltage signal over a zero baseline in light blue. The general behavior is due to the velocity increasing with frequency for some groups of waves.

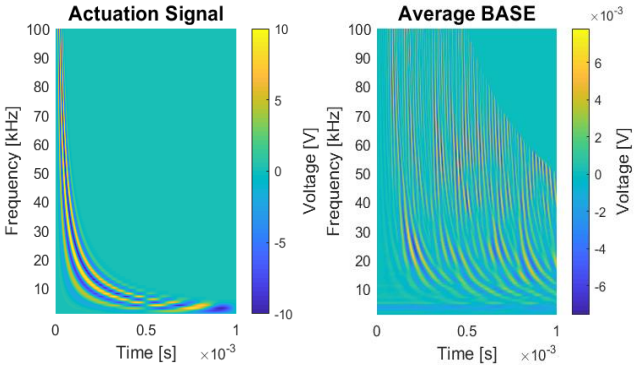

FIGURE 7: SPECTROGRAMS OF BASELINE (LEFT) AND TEST SIGNALS (RIGHT)

As represented in Figure 8, the post-processing of data acquired from piezo sensors in the range of 1-100 kHz has been carried on in two ways:

- analyzing the maximum and minimum peaks at each frequency,
- comparing each value of the Test configuration with the Baseline using the standard deviation.

The first analysis is useful to understand the trend of the signal amplitude along the frequency range, although it is evaluated the local maximum of the signal. From the maximum and minimum Voltage peaks for Baseline, Test 1 and Test 2 configurations it is possible to evaluate a change in the piezo response looking at a line instead of the spectrogram.

The lines at the middle of the graph represent the maximum standard deviation calculated between the 10 signals at each frequency. This value contains the instrumental error for subsequent acquisitions of the same configuration. In fact, it can be noted that under 15 kHz the value of standard deviation is higher than the absolute maximum amplitude of the signal, concluding that in the range 1-15 kHz the signals are not reliable for the SHM system development.

The second analysis is the comparison of the absolute Voltage values for each Test configuration with the Baseline. The Figure 8 shows the three-dimensional graphs for an example of standard deviations used for two comparisons Test 1 with Baseline and Test 2 with Baseline. This type of representation allows to visualize the zones in Frequency and Time domains where the signals acquired in the Test configuration has changed most from the Baseline.

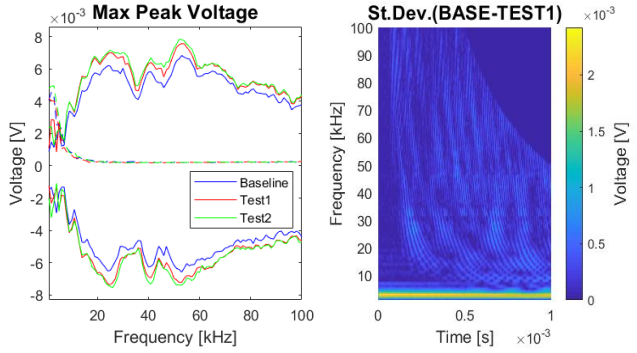

FIGURE 8: MAX AND MIN VOLTAGE PEAKS FOR AN EXAMPLE OF DATA ACQUISITION (LEFT), SPECTROGRAM OF STANDARD DEVIATION (RIGHT)

The main objective of the SHM is to identify a variable that can be used to express the state of integrity of the structure. In case of critical damages or working over the design limits, the value of this variable must increase over a threshold leading to an alarm for the user.

In this paper the algorithms developed by [16] have been applied to the experimental data of specimens and component testing. The Equations (1-6) define the six algorithms used to calculate Damage Index (DI) using the MatLab functions.

The algorithms CCA, CC0, CRC are based on the cross-correlation between two series of signals. In particular, the MatLab functions used are:

- xcorr that returns the similarity between the first signal and the shifted (lagged) copies of the second signal as a function of the lag,
- corrcoef that returns the correlation coefficient between the two series.

The algorithms NRE, MA e ENV are based on the evaluation of amplitude difference between two series of signals. The square difference, in case of NRE, amplify the gap between the signals at the same time of acquisition. The MA consider the global maximum difference that is not the same of the global maximum of the difference envelope.

CCA: $1 - max(xcorr[x_{ij}(t), y_{ij}(t)])$ (1)
CC0: $1 - xcorr[x_{ij}(t), y_{ij}(t)](0)$ (2)
CRC: $1 - corrcoef[x_{ij}(t), y_{ij}(t)]$ (3)
NRE: $\int_0^T (x_{ij}(t) - y_{ij}(t))^2 \, dt$ (4)
MA: $max[x_{ij}(t) - y_{ij}(t)]$ (5)
ENV: $max[env(x_{ij}(t) - y_{ij}(t))]$ (6)

Figure 9 represents the Damage Index calculation of Test 1 (Damage 1) and Test 2 (Damage 2) configurations respect to the Baseline on the range 1-100 kHz for a single piezo couple. The trend of Damage Index is complex and a uniform methodology to compare them on the entire range of frequency has been chosen. The percentage change of the Damage Index of the Test 2 respect to the Test 1 has been calculated, in order to relate the sensitivity of the DI algorithms with a percentage increment.

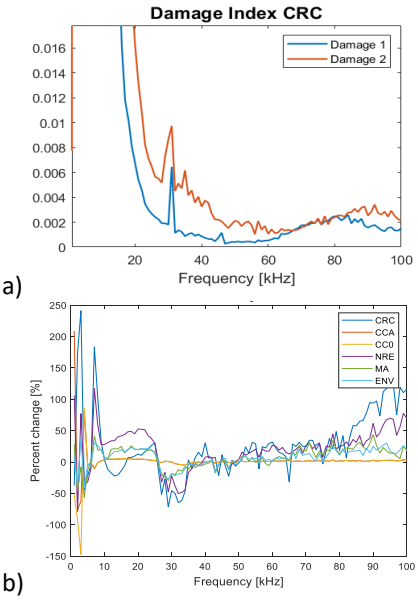

FIGURE 9: a) EXAMPLE OF DAMAGE INDEX OF TEST 1 (DAMAGE 1) AND TEST 2 (DAMAGE 2) CONFIGURATIONS RESPECT TO BASELINE, b) EXAMPLE OF DAMAGE INDEX PERCENTAGE CHANGE FOR TEST 2 RESPECT TO TEST 1

2.4 Virtual Methodology

The FEA simulations have been conducted on LS-DYNA, using LS-PrePost to set the models. The Explicit solver has been used because the vibration phenomenon is time-dependent and its velocity is relatively high. The Implicit solver has not been used because it is normally suitable for quasi-static simulations without a dependence from time.

The modelled structures are the same of the experimental tests. The geometries of specimens, the materials, the thicknesses have been respected. All the piezo sensors on the Top face of the specimens have been modelled. Particular attention has been given to the mesh to preserve the adaptability on large models and the sustainability of computation time.

The Beam specimen has been taken as case study for its simplicity, small dimension and presence of only one piezo couple. Some trials have been carried on using different approaches to model the beam, the piezoelectric, glue and export keywords. It is possible to note in Figure 10 and Figure 11 that the Beam has been modeled as shell 2D, the piezo actuator and sensor as solid 3D, the glue with Tied contact. The polymeric cover, the electrodes and the cables have not been modeled. The mesh has been prepared with square 2D elements of size equal to 1 mm for the beam and with tetrahedron 3D elements of size around 1 mm for the piezo. The dimensions of

the piezo disk were thickness of 0.5 mm and diameter of 10 mm. Tied contact is implemented to model the glue between the beam specimen (master) and the bottom set of nodes of piezo (slaves).

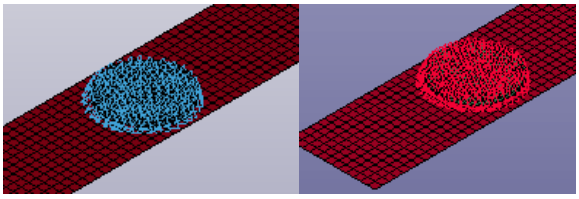

FIGURE 10: DETAILS OF BEAM MODEL: PIEZO 1 ACTUATOR (LEFT) AND PIEZO 2 SENSOR (RIGHT)

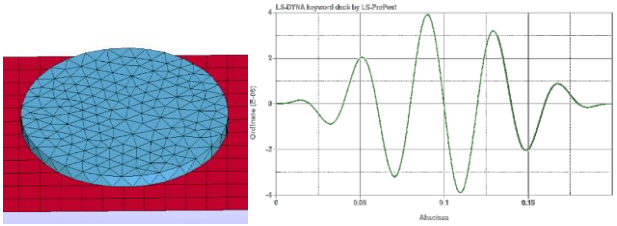

FIGURE 11: MESH OF BEAM SPECIMEN WITH SHELL 2D AND PIEZO WITH SOLID 3D (LEFT), ACTUATION SIGNAL (RIGHT)

The described modelling methodology makes the following approximations:

- Thickness mode vibration of the piezo becomes entirely displacement on the structure;
- Displacement is measured only in 1 node (central node) with *DATABASE_NODOUT;

While have been neglected:

- Radial mode vibration of the piezo;
- Properties of the glue;
- Properties of the Kapton cover of the piezo;
- Real piezo pre-loading due to the Kapton cover;
- Shell 2D elements are used and the propagation of vibrations in the thickness.

The virtual simulations have been conducted at three frequencies of displacement signal: 25, 50 and 75 kHz. In order to optimize and automatize the procedure of model setup for the input signal, the Hanning displacement signal at 50 kHz (Figure 11) was used as a reference using the scale function of LS-PrePost for the other frequencies.

The need of an Electro-Mechanical Coupling is due to the impossibility for LS-DYNA software to evaluate electrical variables, but only mechanical displacement or forces. A specific keyword is under development for the piezoelectric simulation, but it was not available for the use in this work. The theoretical relations of piezoelectricity are based on the properties of piezoceramic material contained in the datasheet of PIC255 material for the DuraAct piezo. The equations for the thickness mode vibration of thin disks were used in this work.

The electrically induced displacement corresponds to the piezo actuator excitation related to voltage by Equation (7) of inverse piezoelectric effect. The “mechanically induced voltage” corresponds to the piezo sensor response signal related to force by Equation (8) of direct piezoelectric effect.

$$\Delta TH[mm] = d_{33}U \cdot 10^3 \frac{mm}{m} \cdot = 4 \cdot 10^{-7} \cdot U[V] \quad (7)$$

$$U[V] = \frac{4 \cdot g_{33} TH}{\pi OD^2} \cdot F_3 = -6.37 \cdot 10^{-2} \cdot F_3[N] \quad (8)$$

Where:

- ΔTH, resulting displacement of the piezo
- U=[-10:10] V, Voltage range used in the tests
- d33=400·10-12 C/N, Piezoelectric charge coefficient in direction 33
- g33=25·10-3 Vm/N, Piezoelectric voltage coefficient in direction 33
- TH=0.2mm, thickness of the piezo core

- OD=10 mm, diameter of the piezo core

For the actuation signal with shape of 5 sines Hanning modulation, the Voltage has been converted to Displacement according to Equation (7) and then applied to the model of piezo actuator with the already explained keyword *BOUNDARY_PRESCRIBED_MOTION_SET.

For the sensor response signal, the Voltage has not been obtained from Force as indicated by Equation (8). In fact, the Voltage values from Force exported using the keyword *DATABASE_NODFOR did not correlate with the Voltage values from experimental tests. This could be for one of the approximations of the model listed before. The incongruence has been fixed with an empiric analogy, especially studied for the beam specimen and then validated on the other specimens.

The relation bases on the replacement of Force with Displacement in the electro-mechanical coupling to calculate the electrical Voltage. Two coefficients have been used to scale the amplitude of actuator and sensor signals, while the time scale is conserved. The scale factor SF has been applied to the same Equation (7) of the actuator signal. The coefficient K has been applied to the inverse of Equation (8) for the sensor signal.

The scale factor SF was designed to calibrate the actuation signal, in the transmission of vibration from piezo actuator to the structure. It has been calculated for each specimen, material and frequency.

The coefficient K was designed to calibrate the received signal, in the transmission of vibration from structure to the piezo sensor. A special test has been prepared joining two piezoelectric patches together with the same glue used on the beam and maintaining the same thickness. One piezo was the actuator and one the sensor, with the same modulated signal, as reported in Figure 12. A simple LS-DYNA model has been set in order to compare real and virtual results, corrected changing the coefficient K. The green circle of Figure 13 is the zone of best fitting, found in the first sinusoid to avoid reverberances of the vibrations between the two piezo.

An example of result obtained from the developed methodology for the numerical-experimental correlation of Voltage signals is reported in Figure 14.

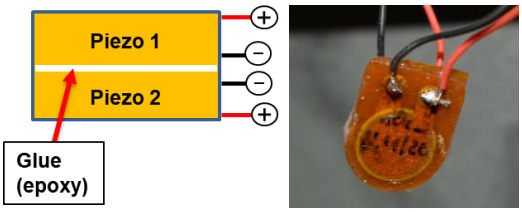

FIGURE 12: SCHEME OF THE SPECIAL TEST (LEFT), DETAIL PICTURE OF THE PIEZO JOINING (RIGHT)

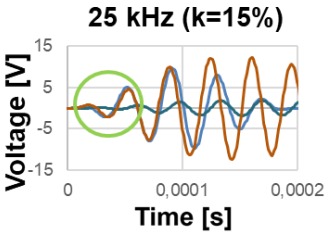

FIGURE 13: SENSOR RESPONSES FROM TEST AT 25 KHZ

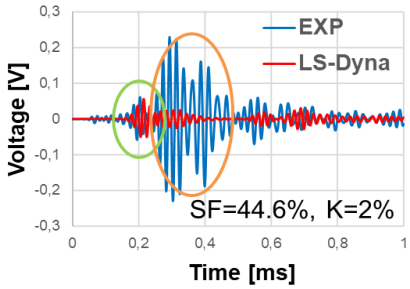

FIGURE 14: NUMERICAL-EXPERIMENTAL CORRELATION OF VOLTAGE SIGNALS FROM PIEZO SENSOR

RESULTS AND DISCUSSION

3.1 Experimental Results

In Figure 15 are reported the Percentage Variations of Damage Index of Damage 2 to No Damage respect to Damage Index of Damage 1 to No Damage for PZT 1-2 piezo couple.

Especially for the Beam specimen made of Steel, it is possible to state that Clamped configuration leads to a general increase of Damage Index value respect to Appended one.

For all the materials investigated, for the Algorithms CRC, NRE, MA, ENV at the frequencies 35 kHz and around 90 kHz, there is a peak related to the detection of the Damage 2 (passing hole diameter 4 mm) respect to Damage 1 (surface indentation diameter 2 mm). For the Algorithms CCA, CC0 there is not a common behavior within the materials.

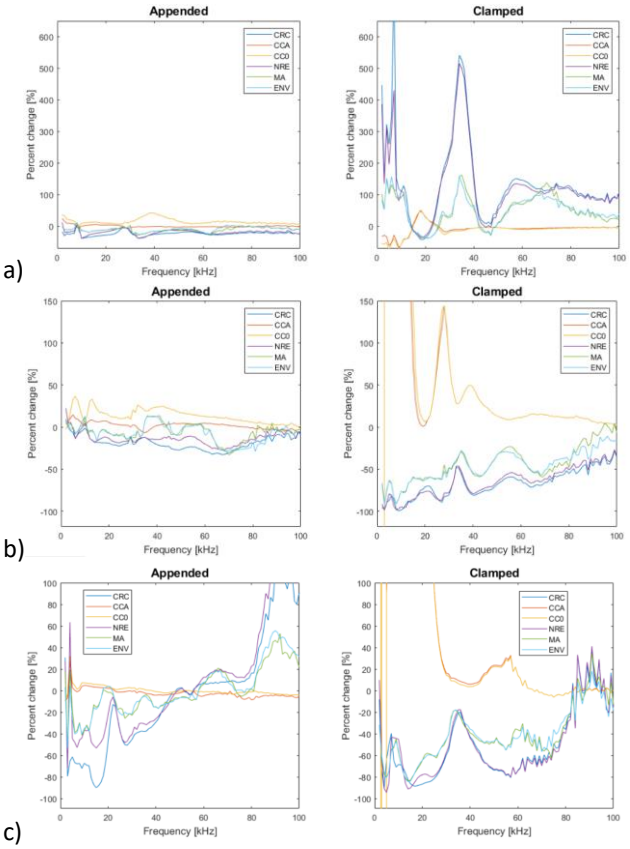

FIGURE 15: SHM TEST RESULTS FOR BEAM a) ALUMINUM, b) STEEL, c) CARBON FIBER

In Figure 16 are reported the Percentage Variations of Damage Index of Plate with Damage 2 to No Damage respect to Damage Index of Damage 1 to No Damage for PZT 1-2, PZT 1-3, PZT 1-4 piezo couples.

For all the materials investigated, in particular for the Algorithms CRC, NRE, MA, ENV, a great increase of Damage Index has been registered related to the detection of the Damage 2 respect to Damage 1. Especially for the Plate specimen made of Carbon Fiber, it is possible to identify two peaks at about same frequencies found for the Beam, 35 kHz and 90 kHz.

Regarding the different Piezo sensors, have a considerable influence of the Damage severity increasing on the Damage Index of PZT 2 and PZT 3 respect to PZT 4. This confirms the initial hypothesis of Damage interaction on the Piezo response when it is on the path of the piezo couple actuator-sensor.

To explain the major Damage Index related to PZT 1-3 respect to PZT 1-2, it is necessary to observe the distance of the two piezo couples. The distance between PZT 1-3 is 200 mm at 0° direction, while for PZT 1-2 is 140 mm at 45°. The waves from actuator PZT 1 reach first the sensor PZT 2, a part of these reflect to the edge of the plate and reach the sensor PZT 3 together with the waves on the

direct path of PZT 1-3. In this way, the influence of the Damage is amplified on the Plate specimen due to reflections of the waves on the edges, leading to a greater Damage Index for couple PZT 1-3 than PZT 1-2.

a)

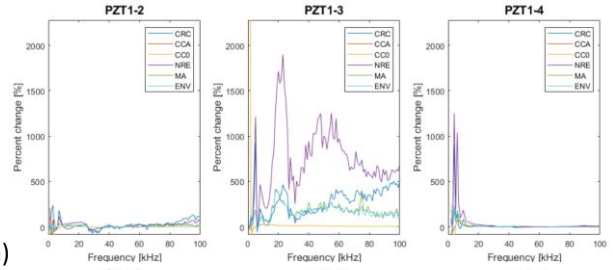

b)

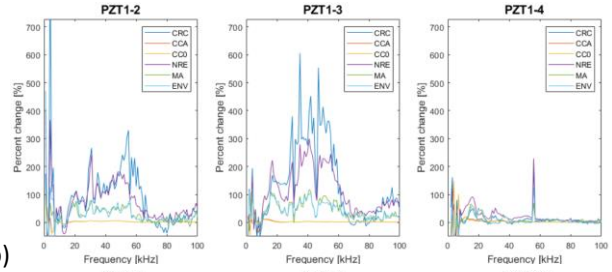

c)

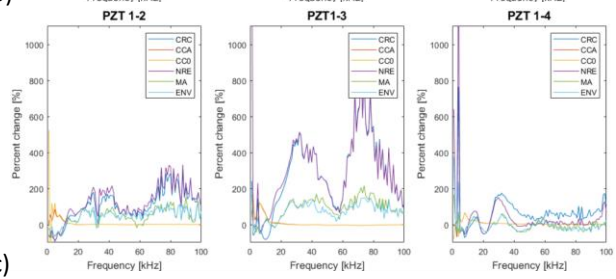

FIGURE 16: SHM TEST RESULTS FOR PLATE a) ALUMINUM, b) STEEL, c) CARBON FIBER

In Figure 17 and Figure 18 are reported the Percentage Variations of Damage Index of BEND2 to BEND0 respect to Damage Index of BEND1 to BEND0 in the three damage conditions, for the Simulacrum specimens made of Aluminum, Steel and Carbon Fiber for PZT 1-2 and PZT1-3 piezo couples.

For all the materials investigated, both piezo couples PZT 1-2 and PZT 1-3 showed interesting behavior for Damage Indexes processed with Algorithm CRC and NRE, so hereby are reported the observations only for these two Algorithms.

It can be noted that, for all the configurations and Damage conditions, the Bending step 2 leads to a higher Damage Index than Bending step 1, in fact there is always a positive percentage variation. This demonstrates that the stresses into the structure affect the final results of the SHM system, so they have to be considered for each application.

Furthermore, the Damage condition of the specimen affect the variation of Damage Index between Bending step 2 and step 1, resulting in a progressive growing trend. In the wide range of 1-100 kHz, over 50 kHz some peaks can be highlighted for all the tests, in particular the frequency of 75 kHz showed the most sensitivity to bending load changes and damage severity increasing.

a)

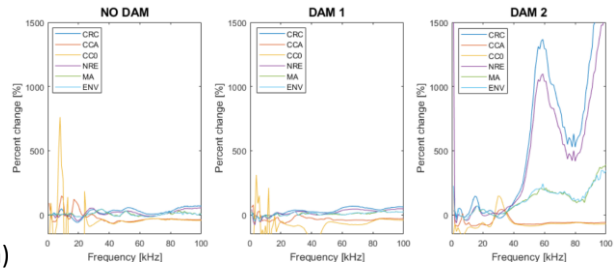

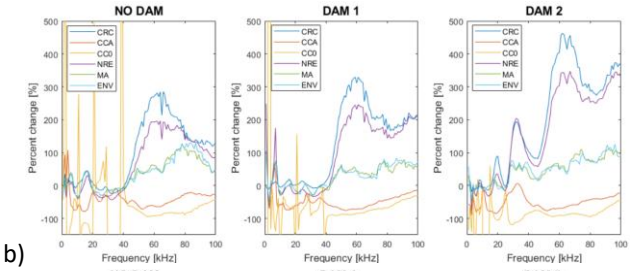

b)

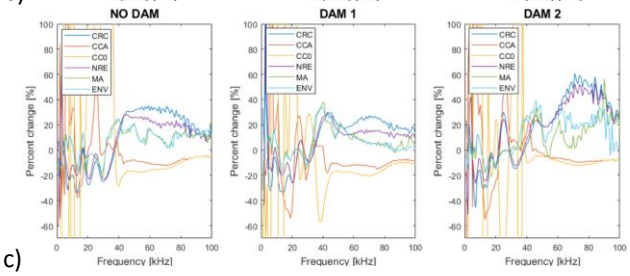

c)

FIGURE 17: SHM TEST RESULTS FOR PIEZO COUPLE 1-2 ON SIMULACRUM a) ALUMINUM, b) STEEL, c) CARBON FIBER

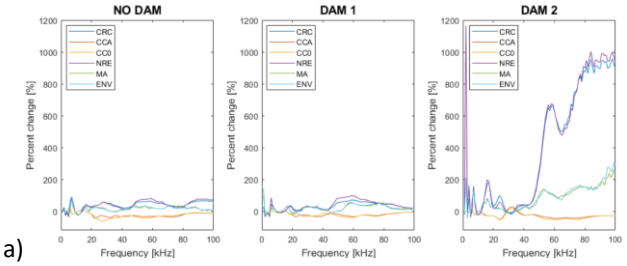

a)

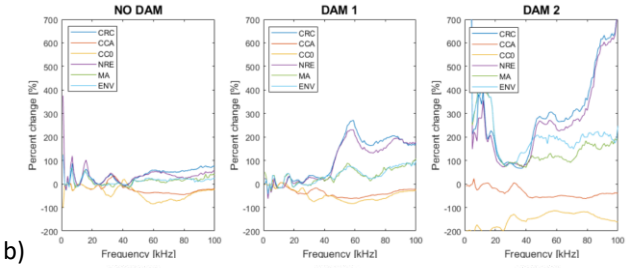

b)

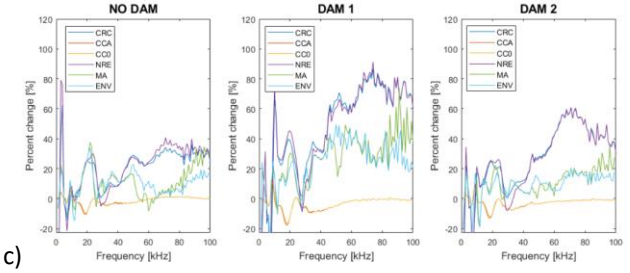

c)

FIGURE 18: SHM TEST RESULTS FOR PIEZO COUPLE 1-3 ON SIMULACRUM a) ALUMINUM, b) STEEL, c) CARBON FIBER

3.2 Simulation Results

Figure 19 describes the evolution of wave propagation, in particular: a) actuation begins and waves spread in two directions, b) wave reflects on the edge opposed to piezo sensor, c) 1st wave reaches the piezo sensor. The FEM model simulates accurately the time of the 1st wave for all the frequencies, as reported in Figure 20.

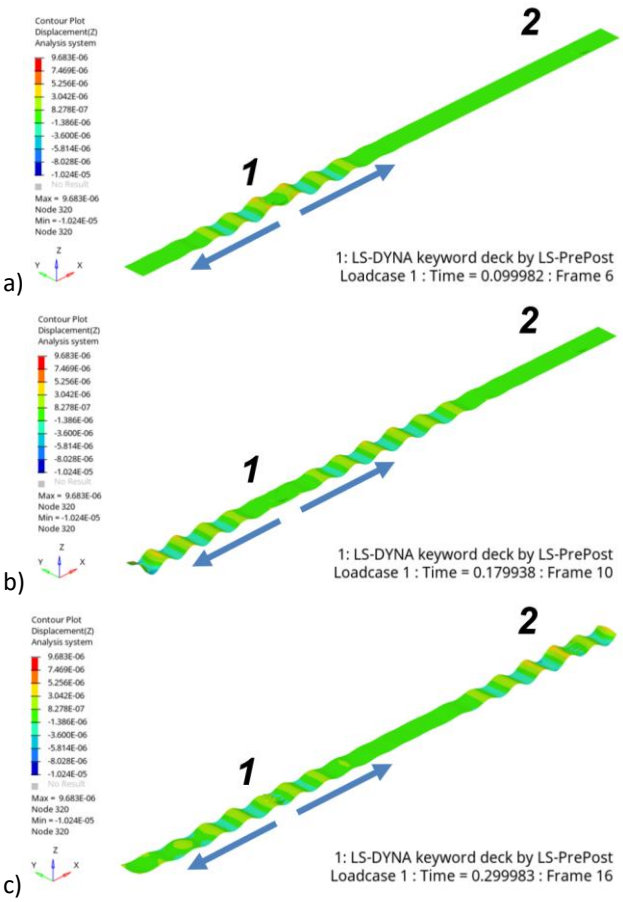

FIGURE 19: WAVE PROPAGATION ON CFRP BEAM AT 25 KHZ: a) ACTUATION, b) PROPAGATION, c) REFLECTIONS

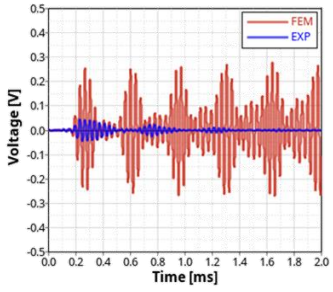

FIGURE 20: NUMERICAL-EXPERIMENTAL CORRELATION OF VOLTAGE SIGNALS FROM PIEZO 2 FOR CFRP BEAM AT 25 KHZ

Figure 21 describes the evolution of wave propagation: a) actuation begins and waves spread uniformly with circular propagation, b) waves reflected on the near edge constructively interfere mainly in x direction and at 45° reaching together piezo sensors 2 and 4, c) while the wave in x direction has completely reflected, the waves on piezo 2 and 4 reflect another time at 45° reaching the piezo sensor 3. Figure 22 reports the Voltage correlations for piezo sensor 2 and 3, that are good for all the frequencies in terms of amplitude and time of arrival of the first waves.

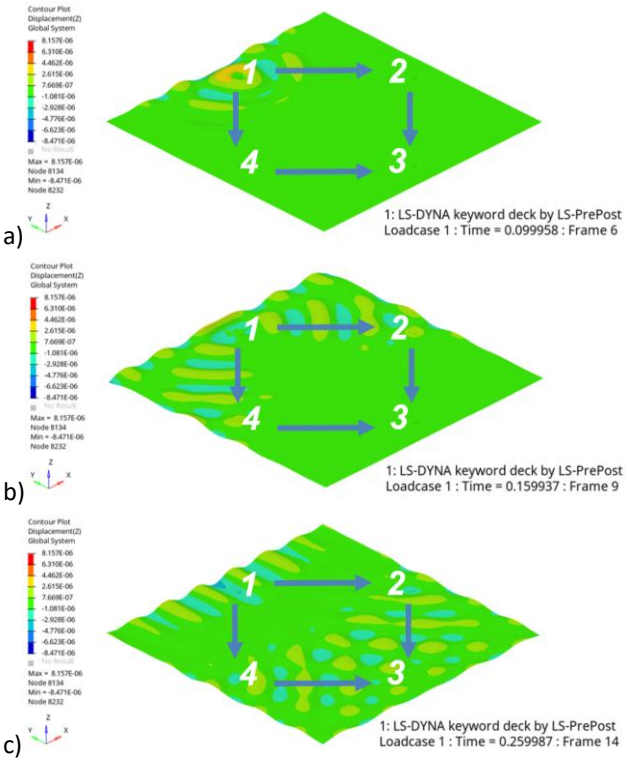

FIGURE 21: WAVE PROPAGATION ON CFRP PLATE AT 25 KHZ: a) ACTUATION, b) PROPAGATION, c) REFLECTIONS

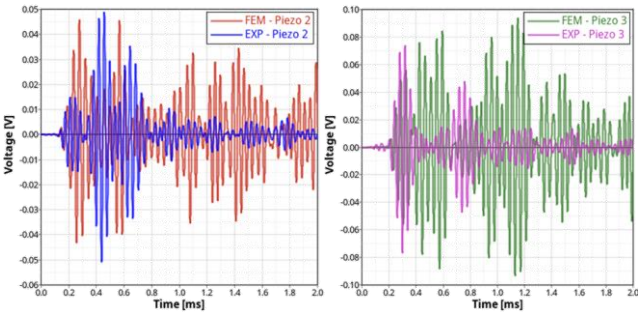

FIGURE 22: NUMERICAL-EXPERIMENTAL CORRELATION OF VOLTAGE SIGNALS FROM PIEZO 2 (LEFT) AND PIEZO 3 (RIGHT) FOR CFRP PLATE AT 25 KHZ

Figure 23 describes the evolution of wave propagation: a) actuation begins and waves spread uniformly with circular propagation reaching the piezo sensor, then the reflections on the edges produce a superposition of waves visible in b), c). As visible in Figure 24, the FEM model simulates accurately the time of the 1st wave for all the frequencies.

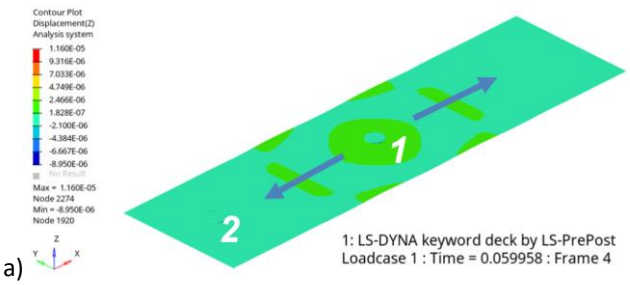

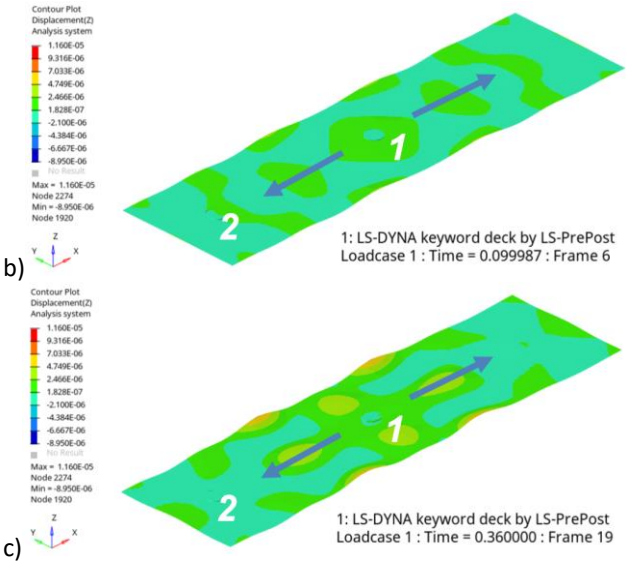

FIGURE 23: WAVE PROPAGATION ON CFRP SIMULACRUM AT 25 KHZ: a) ACTUATION, b) PROPAGATION, c) REFLECTIONS

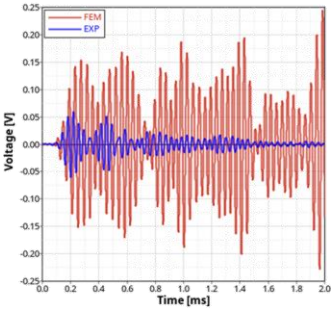

FIGURE 24: NUMERICAL-EXPERIMENTAL CORRELATION OF VOLTAGE SIGNALS FROM PIEZO 2 FOR CFRP SIMULACRUM AT 25 KHZ

CONCLUSION

The main results of the research work are:

- Piezoelectric Sensor response changes with materials, stress condition and damage type;
- Damage Index values must be linked to other measurements (e.g. Strain) when the structure is stressed;
- Frequency of 75 kHz is the most sensitive to Damage and bending load;
- CRC is the preferred Algorithm to monitor Damage and bending load;
- Time of Arrival for waves received from piezo sensors can be simulated in a good manner and can be used in the design phase of the Sensor Network.

The described Damage Index Algorithms need fine tuning and lots of experiments to ensure reliability of the system for application in the Automotive field, but the results obtained in this work are extremely encouraging.

ACKNOWLEDGEMENTS

The authors would like to thank: Simone Reitano, Simone Rabino, Giulia Greco and Victor Hugo Belo Teles for the contribution in this work; Gianluca Poli from Phisik Instrumente (PI) for the support with the DuraAct piezoelectric transducers. The IEHV Research Team benefited from the contribution of the Torino Chamber of Commerce (https://www.dimeas.polito.it/en/research/research_groups/innovative_electric_and_hybrid_vehicles).

REFERENCES

[1] Roach, D., Neidigk, S. Does the Maturity of Structural Health Monitoring Technology Match User Readiness?, in: F.-K. Chang. Structural Health Monitoring 2011 - Condition-Based Maintenance and Intelligent Structures, Volume 1 - 5.1 Introduction of SHM Survey - Background and Motivation. DEStech Publications. 2011.

[2] Carello, M. Airale, A. G. Ferraris, A. Messana, A. Sisca, L. Static Design and Finite Element Analysis of Innovative CFRP Transverse Leaf Spring, Applied Composite Materials. 2017. https://doi.org/10.1007/s10443-017-9596-6

[3] Messana, A. Sisca, L. Ferraris, A. Airale, A.G. Carello, M. Lightweight design of a multi-material suspension lower control arm, Proceedings of the ASME Design Engineering Technical Conference and Computers and Information in Engineering Conference, IDETC-CIE 2020; 17-19 August 2020, Volume 4. https://doi.org/10.1115/DETC2020-22323

[4] Messana A. Sisca, L. Ferraris, A. Airale, A.G. Pinheiro de Carvalho H., Sanfilippo P. Carello, M. From design to manufacture of a carbon fiber monocoque for a three-wheeler vehicle prototype, Materials, Volume 12(3), 2019. https://doi.org/10.3390/ma12030332

[5] Kessler, S.S. Spearing, S.M. Structural Health Monitoring of Composite Materials using Piezoelectric Sensors. 2002.

[6] Ooijevaar, T. Vibration Based Structural Health Monitoring of Composite Skin-Stiffener Structures, Ph.D. Thesis. 2014.

[7] Mitra, M. Gopalakrishnan, S. Guided wave based structural health monitoring: A review, Smart Materials and Structures. 2016. http://dx.doi.org/10.1088/0964-1726/25/5/053001

[8] Carello, M. Ferraris, A. Airale, A.G. Messana, A. Sisca, L. De Carvalho Pinheiro, H. Reitano, S. Experimental Characterization of Piezoelectric Transducers for Automotive Composite Structural Health Monitoring, SAE Technical Papers; Volume 2020(April), 2020. https://doi.org/10.4271/2020-01-0609

[9] Boffa, N.D. Structural Health Monitoring (SHM) systems in aircraft: wing damage detection employing guided waves techniques, Ph.D. Thesis. 2016.

[10] Bekas, D.G. Sharif-Khodaei, Z. Ferri Aliabadi; M.H. An Innovative Diagnostic Film for Structural Health Monitoring of Metallic and Composite Structures, Sensors. 2018. https://doi.org/10.3390/s18072084

[11] Gianneo, A. Carboni, M. Giglio, M. Feasibility study of a multi-parameter probability of detection formulation for a Lamb waves–based structural health monitoring approach to light alloy aeronautical plates, Structural Health Monitoring. 2017. https://doi.org/10.1177%2F1475921716670841

[12] Gorgin, R. Luoa, Y. Wu, Z. Environmental and operational conditions effects on Lamb wave based structural health monitoring systems: A review, Ultrasonics. 2020. https://doi.org/10.1016/j.ultras.2020.106114

[13] Loutas, T.H. Charlaftis, P. Airoldi, A. Bettini, P. Koimtzoglou, C. Kostopoulo,s V. Reliability of strain monitoring of composite structures via the use of optical fibre ribbon tapes for structural health monitoring purposes, Composite Structures. 2015.

[14] Güemes, A. Fernandez-Lopez, A. Pozo, J. Sierra-Pérez, A.R. Structural Health Monitoring for Advanced Composite Structures: A Review, Journal of Composites Science. 2020. https://doi.org/10.3390/jcs4010013

[15] Wang, C.S. Wu, F. Chang, F.-K. Structural health monitoring from fiber-reinforced composites to steel-reinforced concrete, Smart Materials and Structures. 2001. https://doi.org/10.1088/0964-1726/10/3/318

[16] Mechbal, N. Rebillat, M. Damage indexes comparison for the structural health monitoring of a stiffened composite plate, 8th ECCOMAS Thematic Conference on Smart Structures and Materials. 2017.